SECTION 1
DATA AND CORRELATION

1

Equilibrium Water Content Measurements For Acid Gas Mixtures

R. A. Marriott[1], E. Fitzpatrick[2], F. Bernard, H. H. Wan, K. L. Lesage, P. M. Davis, and P. D. Clark

[1]*Alberta Sulphur Research University of Calgary*
Calgary, AB, Canada
[2]*Deceased September 29, 2008*

Abstract

Understanding the acid gas and water equilibrium is an important aspect for designing safe and reliable injection facilities. For example, (i) accurate prediction of water content is important for multiple stage compression of high-CO_2 and/or high-H_2S process gases to dense phase injection fluids and (ii) predictive models are of interest for reservoir simulation at much higher pressures. While several studies have been conducted on water content data for pure CO_2 and some data published for pure H_2S, there has been a limited investigation into the water content of acid gas mixtures at high pressure. The scarcity of data is due, in large part, to the experimental difficulty in obtaining representative samples of equilibrated dense phase acid gases (liquids and supercritical fluids).

In collaboration with the Schulich School of Engineering, University of Calgary, ASRL has conducted a joint industry project to measure water contents for acid gas mixtures under moderate pressures and temperatures (T = 25 to 60°C and p = 10 to 150 bar). To date, ASRL has reported over 160 data points, which constitutes more than half of those available in the public literature. Over the last 8 years ASRL has used several techniques to obtain these measurements; these include: (1) visual dew point determination for liquid acid gas + hydrates, (2) equilibration of samples in stirred autoclaves, (3) basic static equilibration cells, and (4) an isolated floating piston with a micro-sampler for near-direct GC injection of gaseous or liquid acid gas phases. The evolution, advantages and disadvantages of these techniques will be described.

Wu/Carroll (ed.) Acid Gas Injection and Related Technologies, (3–20)

Finally, as the Joint Industry Project was coming to an end, the micro-sampling technique also evolved in capability. The high-pressure limit is now 1000 bar, which includes nearly any injection reservoir pressure under consideration for commercial application. Note that 0 – 100 % H_2S can be accommodated. Among the current ASRL projects is the investigation of pure H_2S + water equilibria at very high pressures and the testing of a new Thermioinic GC detector (TID-1) which is tuned for water. These new techniques and some recent data will be summarised within this presentation. Full data sets are available with in the ASRL quarterly bulletin.

1.1 Introduction

Several papers have addressed the importance of accurate predictions for the water content of both sour gas and acid gas [1, 2]. In particular, the design of a safe acid gas injection project requires that the phase behavior involving H_2S, CO_2 and H_2O be well characterized [3, 4]. Many models have addressed this characterization; however, historically there has been a lack of experimental water content information for the H_2S + CO_2 acid gas mixtures, particularly in the liquid acid gas region [1, 3, 5]. These data are useful for verifying the interpolation accuracy of existing models and/or calibration of newer models.

The primary utility in wet acid gas phase behavior modelling, is in understanding and describing the effectiveness of compression cycles for partial dehydration or dewatering [4, 6]. Substantial cost savings are available if an acid gas can be transported from compression to injection without formation of free water or production of a hydrate phase, *e.g.*, free water leads to increased corrosion rates. Thus, acid gas leaving a compressor facility is often designed to be under saturated with water for all downstream conditions. The alternative would include dehydration by glycol or molecular sieve. For illustration of how the compression cycles can be used to partially dehydrate an acid gas, the phase behavior of a 50:50 H_2S/CO_2 acid gas is shown in Figures 1a and 1b along with a simplified four cycle compression scheme and water dew point curves [7, 8]. In order to simplify the diagram, the compression profile is unrealistically efficient, the hydrate formation curve has not been included (compression scheme is above T = 40°C), and the inlet gas contains 2% H_2O which is closer to second stage suction saturation conditions. As illustrated in the second and third inter-stage cooling, the water content is reduced from 2.0 to 0.7 % H_2O and 0.7 to 0.3% H_2O (Figure 1b).

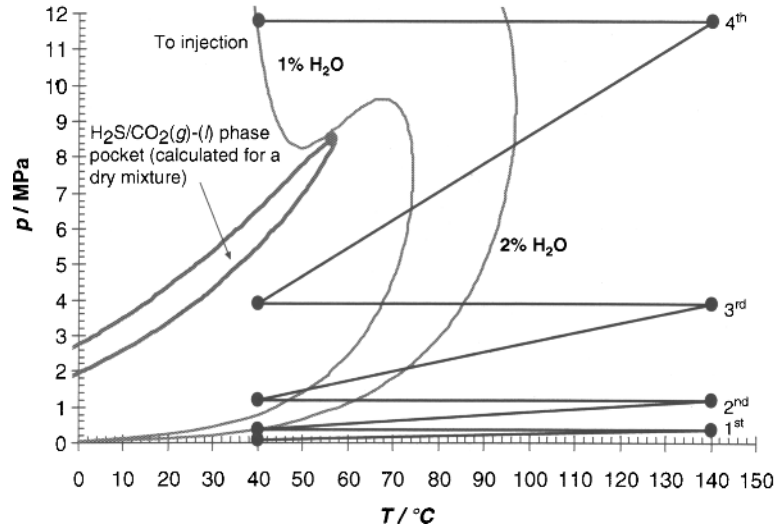

Figure 1a. A simplified schematic for four stages of compression of a 50:50 H_2S/CO_2 acid gas mixture with the 2% and 1% H_2O dew points.

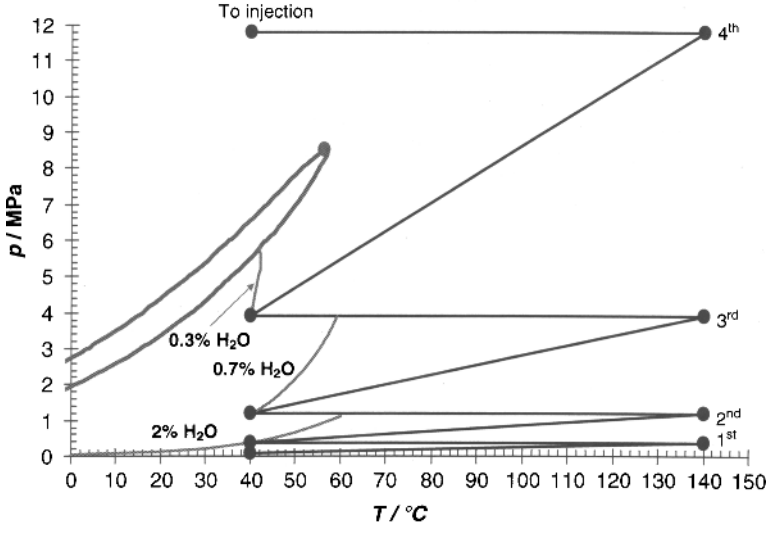

Figure 1b. A simplified schematic for four stages of compression of a 50:50 H_2S/CO_2 acid gas mixture showing the estimated drop in dew point at each suction scrubber condition.

Upon cooling after the 4th stage compression cycle, the 0.3% fluid is well below the water carrying capacity of 1% H_2O (at conditions labeled 'to injection'). Of course in a real design situation, all conditions downstream of the compression would have to be considered.

For example, the fluid pressure profile may drop or rise before entering the wellhead and descending the wellbore [6]. Even the degree of subsaturation in the near wellbore region may be of interest to reservoir modeling, since the fluid likely will have the capacity to take up additional reservoir water.

The phase behavior shown in Figures 1a and 1b is not available within many off-the-shelf software packages. Aqueous equilibria are difficult to model, especially when they involve gaseous, acid gas liquids and supercritical acid gas phases. As previously discussed, experimental water content information for dense phase H_2S + CO_2 acid gas mixtures is not available in the open literature; therefore, any model must be parameterized with water content data for CO_2 and sparse published data for pure H_2S. Water contents for non-liquid mixtures containing acid gases (sour gases) have been reported by some authors.

In 2001 ASRL began work with the researchers in the Schulich School of Engineering under a joint industry project aimed at measuring water contents for acid gas mixtures under moderate pressures and temperatures (T = 25 to 60°C and p = 10 to 150 bar). The intent of this paper was not to report all the data measured to date; rather, it serves to communicate lessons learned and the story of ASRL's measurement improvements throughout the process of completing a very ambitious experimental matrix. The evolution of these techniques was driven by the same phase behavior shown in Figures 1a and 1b. Finally, the most recent data set for 50:50 H_2S/CO_2 mixture is presented and compared against previous data.

The dry phase pockets have been calculated using VMGSim 2.8.0 [7] and the water dew point phase pockets have been calculated using AQUAlibrium 3.0 [8].

The dry phase pockets have been calculated using VMGSim 2.8.0 [7] and the water dew point phase pockets have been calculated using AQUAlibrium 3.0 [8].

1.2 Available Literature Data

Both experimental data and theoretical treatments for the water contents of pure acid gases and their mixtures have been reviewed by Carroll [5] and Clark [1]. More recently, Chapoy et al. [9, 10] have reviewed the experimental water content data available for

pure CO_2 and H_2S. The conditions for the CO_2 water content data [11–21] have been shown in Figure 2a and the conditions for H_2S water content data [10, 12, 22–23] have been shown in Figure 2b. Comparing figure 2a and 2b shows that there is much more experimental data available for the CO_2 system than for the H_2S system. Surprisingly, even with the abundance of CO_2 data, there are few data for the conditions of $p > 20$ MPa and $T > 75$°C and many acid gas target reservoirs or CO_2 sequestration reservoirs would fall into this temperature and pressure range. For H_2S, Figure 2b, there are no data above *ca.* 30 MPa and experimental data in the liquid H_2S region are mostly those of Gillespie and Wilson [12]. The reasons for the limited studies in this region are (1) the toxicity of H_2S makes high pressure H_2S experimental work difficult and (2) sampling the system is challenging due to the change in water solubility as the fluid is depressurized. The latter challenge will be discussed further.

For mixtures containing both CO_2 and H_2S, Huang *et al.* [24] have published 16 measurements for mixtures of 10:30:60 $H_2S/CO_2/CH_4$ [p = 4.8 – 17.3 MPa, T = 37.8 – 176.7 °C] and 80:10:10 80:10:10 $H_2S/$

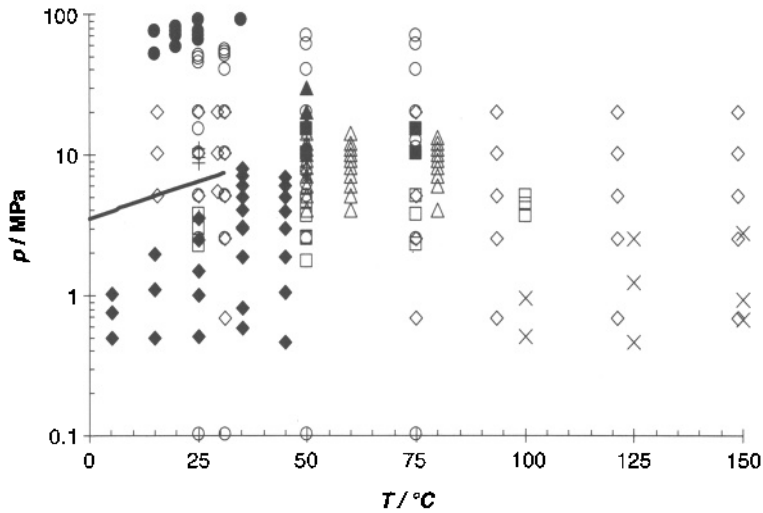

Figure 2a. Conditions for CO_2 water content data reported in the literature. °, Wiebe and Gaddy; [11] ◇, Gillespie and Wilson; [12] □, Coan and King; [13] •, King *et al.*; [14] ×, Zawisza and Malesińska; [15] ■, D'Souza *et al.*; [16] ◆, Valtz *et al.*; [17] ✱, Briones *et al.*; [18] +, Nakayama *et al.*; [19] ▲, Dohrn *et al.*; [20] △, Bamberger *et al.*; [21] —, vapour pressure from the Span and Wagner EOS. [25] Note that the conditions for the Sidorov *et al.* [26] and Müller *et al.* [27] data are missing from this figure.

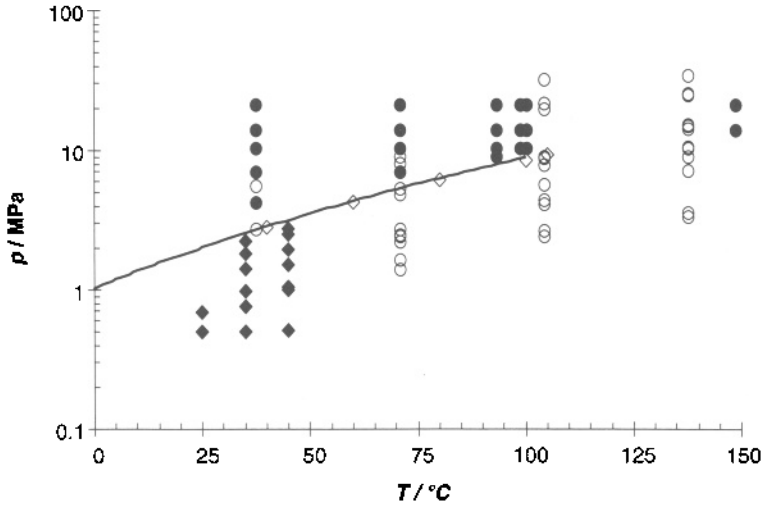

Figure 2b. Conditions for H_2S water content data reported in the literature. ◆, Chapoy *et al.*; [10] •, Gillespie and Wilson; [12] ◇, Carroll and Mather; [22] °, Selleck *et al.*; [23] ——, vapour pressure from the Lemmon and Span EOS [28]. Note that the conditions for the Wright and Maass [29] and Lee and Mather [30] data are missing from this figure.

CO_2/CH_4 [p = 7.6 – 18.2 MPa, T = 37.8 – 176.7 °C]. Clark [1] has measured 91 water contents for several acid gas mixtures ranging from 10-75 mol% H_2S and 15-90 mol% CO_2. Of these available data, 28 are in a liquid acid gas p-T region and 9 are in the supercritical region. It is the liquid and supercritical region which has the largest influence upon any model parameterization, *i.e.*, the water contents in the gas phases (lower pressures/densities) are less influenced by composition or density differences and are easier to model. Figure 3 shows three water dew point curves using three different models [2, 7, 8] of a 50:50 H_2S/CO_2 acid gas mixture. The water dew point curves show deviation in both the liquid and supercritical regions, while all three models agree in the gaseous region.

ASRL's original experimental matrix included acid gases targets from 10 to 90 mol% H_2S and CO_2, with over half of the anticipated conditions in the hydrate, liquid or supercritical regions. 153 measurements were released to the ASRL membership in 2007 [31] and an addition 30 were released to the ASRL membership in 2008 [32]. Currently, ASRL has plans to issue a final report containing another 22 experimental points. Table 1 shows the current conditions

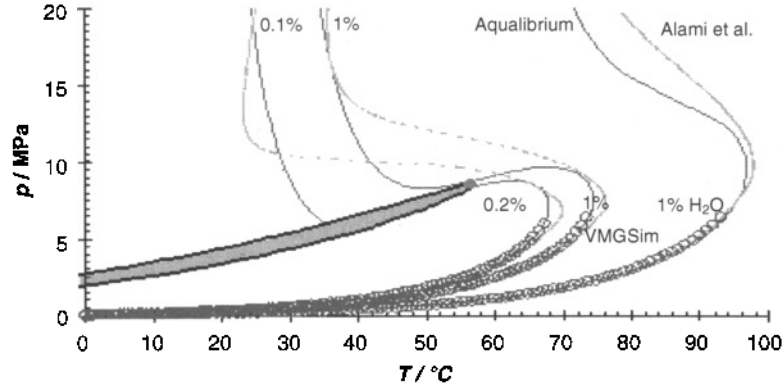

Figure 3. The water dew point curves for a 50:50 H2S/CO2 acid gas mixture calculated using three different models. The dry phase pocket (shaded) has been calculated using VMGSim 2.8.0;[7] _____, water dew point from AQUAlibrium 3.0;[8]. -----, water dew point from Alami *et al.* [2] and °, water dew point from VMGSim 2.8.0.[7]

and maximum H_2S contents available in that database of water content information.

1.3 Equilibration Vessels / Techniques

ASRL has used four distinguishable techniques to obtain water content data for acid gases in the gaseous, hydrate, liquid and supercritical region. These four techniques have been classified as follows:

Table 1. Experimental water content data for acid gas mixtures.

Data Source	n	T (min) °C	T (max) °C	p (min) MPa	p (max) MPa	x_{H_2S} (min) mol%	x_{H_2S} (max) mol%
M.A.Clark [1]	91	–1.3	98.5	0.77	37.9	1.2	85.9
Huang *et al.* [24]	16	37.8	176.7	4.82	18.2	9.4	81.0
ASRL SA [31, 32]	42	30.0	90.0	2.00	10.0	20.0	80.0
ASRL EQ [31, 32]	62	24.6	60.8	1.21	7.85	9.3	89.6
ASRL VDP [31, 32]	10	9.0	23.0	4.65	10.5	48.1	50.0
ASRL IFP/μS [31, 32]	91	39.9	60.1	2.03	19.95	7.3	89.5
Total	312	–1.3	176.7	0.77	37.9	1.2	89.6

(1) a visual dew point cell, VDP, applied in the hydrate *p-T* region; (2) a stirred autoclave, SA, applied in the gaseous *p-T* region; (3) a basic equilibrium cell, EQ, applied in the gaseous *p-T* region; and, (4) an isolated floating piston with a micro sampler, IFP/μS, applied in the liquid and supercritical *p-T* region. These techniques are a result of the evolution of the research.

1.3.1 The Visual Dew Point Cell, VDP

Dieters and Schneider [33] classify two major methods for measuring vapour liquid equilibria as 'synthetic' and 'analytic'. A synthetic method is where a fluid of known composition is synthesized in a vessel and conditions can be changed to induce phase separation. This is an *in-situ* method which does not destroy any portion of the sample. For an example, if one wanted to measure the conditions for the phase pocket shown in Figure 3, they could synthesis a 50:50 H_2S/CO_2 mixture at T = 50°C and p = 10 MPa in a floating piston type vessel. This mixture could then be expand at T = 50°C until a bubble point is detected by a various techniques, including a pressure inflection/halt, enthalpy changes, density changes or visual changes. A similar technique could be used to measure water dew points, *e.g.*, cold finger/mirror technique.

Synthetic techniques are commonly used to detect high pressure hydrates, normally visually or calorimetrically. ASRL uses a high pressure visual cell with sapphire windows. Synthetic fluids are gravimetrically made in larger cylinders (*ca.* 100 cm^3) by charging $H_2O(l)$, $H_2S(l)$ and $CO_2(l)$ respectively. Water is charged using a syringe, $H_2S(l)$ is delivered using a liquid floating piston at 6.9 MPa and CO_2 is delivered using a similar floating piston at 10.3 MPa. Fluids are then heated and expanded into a visual cell (single phase). The cell is immersed in a glycol bath and is cooled below the hydrate temperature to induce hydrate formation. The temperature of the cell is then slowly raised until the hydrate disappears (melts). Note that hydrate formation can be limited by nucleation and growth kinetics, whereas, the hydrate melt is only limited by diffusion. Therefore, a slow heat results in reproducible melting temperature and pressure. Figure 4 shows several video captures of a hydrate being melted. The fluid in the cell was composed of 50:50:0.42 mol% $H_2S/CO_2/H_2O$.

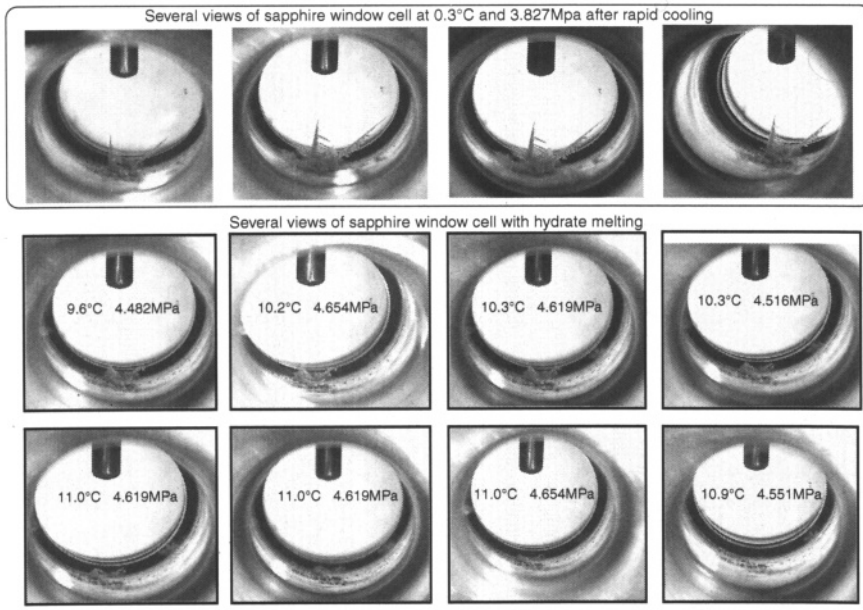

Figure 4. Photographs of a controlled hydrate melt within a sapphire window cell containing 50:50 H_2S/CO_2 acid gas mixture (0.42mol% H_2O).

1.3.2 The Stirred Autoclave, SA, and Basic Equilibrium Cell, EQ

Both the stirred autoclave and static equilibrium cell techniques were used for the liquid water / gaseous acid gas *T-p* regions. Conditions in these regions were easier to achieve, because of the gas compressibility.

Figure 5 shows a schematic of the stirred autoclave and basic static equilibrium cell. For the stirred autoclave, acid gas was delivered until the composition of the outlet acid gas phase was consistent with the inlet composition, *i.e.*, at this point the aqueous phase was saturated. A superheated sample of the vapour was then removed for analyses. Any pressure drop can be compensated by addition of more feed gas. The advantages of this technique are that the temperature, pressure and acid gas composition are well targeted. The disadvantages are that the technique is slow and consumes large quantities of acid gas.

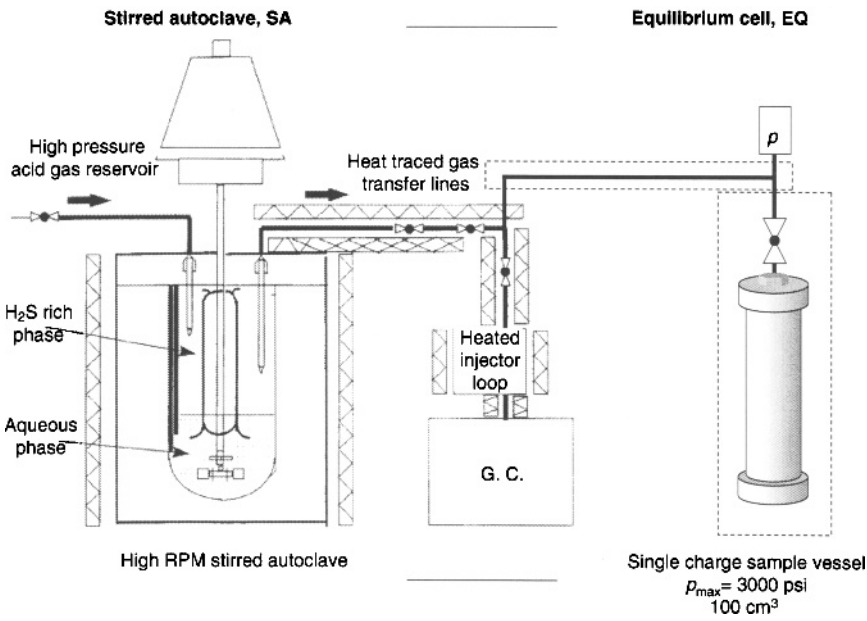

Figure 5. Schematic of the stirred autoclave and basic equilibrium cell technique.

The basic or static equilibrium cells involved a single charge of excess water and acid gas components (measured gravimetrically). After several days of constant heat and gentle agitation, the sample was opened to a small volume transducer to measure the final pressure. The head space (acid gas phase) was then sampled in small volumes to minimize the pressure drop in the vessel ($\delta p < 0.2$ MPa). The advantages of this technique are that it consumes less acid gas, requires very little equipment to perform parallel experiments and it can provide the composition of the aqueous phase by mass difference, if the densities of both phases and the total volume of the vessel are well known. The disadvantages are that it is difficult to simultaneously target temperature, pressure and acid gas composition. In addition, the sampling of these vessels involves throttling the vapour across a hot needle valve to introduce a sub-sample into the GC sampling loop at atmospheric pressure. In some cases the throttling was not consistent and water either didn't make it to the GC or a large slug of water entered the GC with the next sample. Normally 10-12 GC analyses were averaged for every equilibrium point.

1.3.3 The Isolated Floating Piston with Micro Sampler, IFP/μS

In the later stages of the JIP, several improvements were made to the equilibrium cell technique in order to make measurements in the liquid acid gas region. As pointed out previously, the disadvantages of the equilibrium cell technique were that the simultaneous targeting of temperature, pressure and acid gas composition were difficult. Targeting temperature and pressure is much more difficult with a liquid-liquid system where the temperature induced pressure changes are more difficult to anticipate. In addition, to reduce any pressure drop the sample size must be very small, because the fluid is high density. The schematic of the improved equilibrium cell is shown in Figure 6.

The new equilibrium vessel is equipped with a dedicated transducer such that the pressure measurement is always monitored and the equilibration pressure can be better targeted. A floating piston was added to facilitate targeting specific equilibrium pressures. The floating piston is normally isolated during the equilibration time to reduce the need for an additional ballast fluid. The sampling was provided by a block and flow type system between two zero volume HPLC valves (SSI). Each sample reduces the overall pressure by less than 0.02 MPa. Up to 15 samples can be removed for GC analyses. Another significant advantage over the basic equilibration

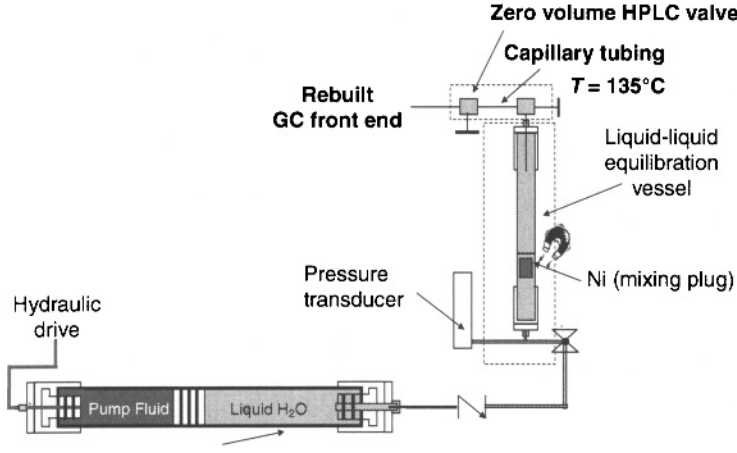

Figure 6. A schematic of the isolated floating piston with micro sampler.

cell is that the system is no longer only a single charge system, since the pressure can be adjusted after each equilibration condition is measured; therefore, several equilibration points can be achieved with one acid gas charge.

1.4 Water Analysis

The latter three techniques used by ASRL are considered analytical techniques which require removing either liquid, supercritical or gaseous fluids from a high pressure cell or autoclave. For the most part, these types of measurements have been well documented in the literature for high pressure hydrocarbon gases. The water content can be measured by adsorption of water in a liquid or solid stationary phase. For liquid adsorbents, Karl-Fischer Titration can be used to for analysis. For solid adsorbents, water can be measured gravimetrically assuming the other components (H_2S, CO_2, etc.) do not absorb. For examples, Weibe and Gaddy [P_2O_5], [11] Selleck *et al.* [$CaSO_4$], [23] and Gillespie and Wilson [$Mg(ClO_4)_2$] [12] all used solid adsorbents to selectively quantify water.

Like many other researchers, ASRL have chosen to analyse for water using Gas Chromatography, GC. The same technique is used to measure the other components in the fluid; therefore, good chromatographic separation is necessary. During the initial stages of research, custom made molecular sieve columns were used. More recently a Restek UPlot column and a thermal conductivity detector have been used. Currently, a CP-PoraBOND U column is being used with a TCD detector and a parallel Thermionic Detector, TID-1-N_2. The U-plot column and bonded UPlot columns provide good polar separation so that H_2O, CO_2, H_2S, COS, N_2, and most hydrocarbons can be separated and analysed in one stream (helium carrier at 20 cm^3 min^{-1}; column T = 40°C with a delayed temperature ramp to T = 190°C).

The TID-1-N_2 (DETector Engineering & Technology, Inc.) currently is being explored for compositions where water is not distinguishable, *e.g.*, with the PlotU column butane and water eluted at the same time. The TID-1-N_2 is a nitrogen/phosphorous detector, NPD; however, it has been tuned to respond selectively to oxygen. Preliminary studies have shown that response degrades over time and that it has a very good response to H_2S. Fortunately, the bonded UPlot column does separate butane and water.

1.5 Sampling Issues for Analytic Methods

The most important and challenging aspect of an analytical water content measurement is the transmission of the high-pressure sample to the low-pressure analytical equipment (GC or adsorption/trap vessel). Samples are accepted for analyses at low pressure; therefore, the liquids must be flashed such that they hold all components, *i.e.*, the water cannot be left behind. This is easier to achieve when one is sampling a gas phase, such as high pressure methane, because as the pressure is isothermally reduced the water carrying capacity increases. Therefore, during the depressurization of high pressure methane + water sample, one needs to overcome the Joule-Thompson cooling effect and no more.

Figure 7 shows the calculated water content for a 75:25 H_2S/CO_2 mixture along several isotherms. Using Figure 7 as an example, one can see that the phase behavior which aids in partial dehydration during compression and cooling, makes the sampling of such a fluid difficult. The liquid or supercritical fluid holds more water than the gas. Eventually the fluid must be at or near atmospheric conditions, even if it is injected directly onto a GC column. As the depressurizing fluid enters the gaseous pressure region, there is a minimum in the water content (true for both supercritical and where there is a liquid to gas transition).

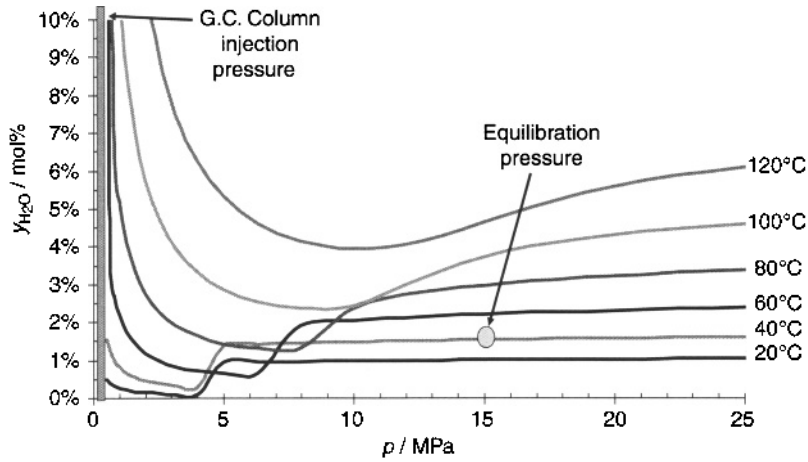

Figure 7. The calculated water content for a 75:25 H_2S/CO_2 acid gas mixture [8].

Therefore, not only does the expansion need to have enough heat to overcome the Joule-Thompson cooling effect, but the liquid must be sampled and heated 40 to 50 °C above it's equilibration temperature.

For example, a 75:25 H_2S/CO_2 fluid equilibrated at T = 40°C and p = 15 MPa must be heated to the 100°C isotherm in Figure 7, before being depressurized. If it were heated to 60°C, the fluid would pass through a pressure range where the water saturation limit would be less than half of what the liquid was actually carrying. Superheating the sample also can create an issue with the temperature control and equilibration conditions. For example, experience shows that if the heat source on a capillary tube is too close to the high pressure vessel, one can establish a local high temperature equilibrium at the tip of the capillary tube (*ca.* 10-20 cm away from the heat source). Thus the water content can be erroneously large if the superheated sample zone is close to the vessel.

Note that each valve operates at T > 125°C. The ten-port valve is Hastelloy 276 and the six-port valve is SS-316.

Once the sample is heated, one option is to inject directly onto the front of the GC column or depressurize into a constant volume and constant pressure injection loop (GC front end). Note that the ROLSI type valve, like the one used by Chapoy, [10] injects through a capillary tubing which is opened for a limited length of time. The carrier gas is passed over the low pressure end of the capillary tubing so that all the sample is directed to the analytical equipment (GC). The capillary-open-time, fluid compressibility and overall pressure in the vessel dictates the volume of gas which is allowed to flow to the GC.

ASRL has chosen to not inject high pressure sample directly, because of the high-pressure and types of fluids involved. In ASRL's case, the volume is always constant regardless of the pressure or fluid type. This procedure has been achieved in two ways, Figure 8. In the first method a sample is throttled across a needle value into a superheated zone. That super heated zone contains a 125 µL injection loop at 0.9 to 0.2 MPa in a six way GC valve. The second method was less difficult and involved less user error. In addition, it has a much larger operating pressure. In this method, the high pressure sample is blocked between two zero volume valves at a much higher temperature than the equilibration vessel. The top

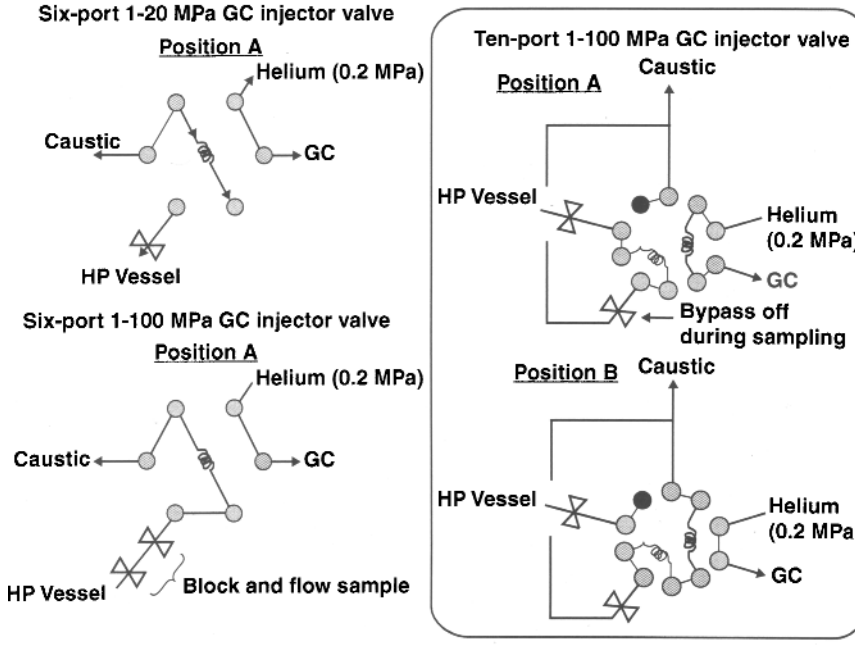

Figure 8. Schematics for three constant volume high-pressure GC injection valves used by ASRL.

valve is then opened and the fluid is slowly flashed/depressurized into the sample injection loop.

Finally, ASRL is now experimenting with a high pressure ten-way injection valve which contains one micro volume high pressure loop and a larger volume injection loop. The goal of this valve is to have automated injection at even hotter temperatures. Results using this new injection valve are not available yet; however, a schematic of the procedure is shown in Figure 8.

1.6 Some Recent Results and Future Directions

After the JIP matrix was fulfilled, we returned to measuring the water contents for the 50:50 H_2S/CO_2 systems. In part, this work was designed to test the reproducibility of our newer sampling techniques and abilities. Data for the T = 40 and 60°C isotherms are reported in Table 2. The T = 60°C data have been shown in Figure 9

Table 2. High-pressure acid gas liquid water content measurements.

T / °C	p / MPa	$y(CO_2)$ / mol%	$y(H_2S)$ / mol%	$y(H_2O)$ / mol%
40.0	8.03	45.2	54.8	1.01
40.1	10.13	50.7	49.3	0.98
40.0	15.02	51.0	49.0	1.02
40.1	15.40	51.1	48.9	1.01
60.0	2.03	44.1	55.9	1.05
60.0	4.01	48.2	51.8	0.69
60.0	5.04	50.3	49.7	0.60
60.0	6.00	51.2	48.8	0.56
60.0	7.03	51.9	48.1	0.57
60.0	7.96	47.0	53.0	0.84
60.0	9.03	50.7	49.3	0.93
60.1	9.98	48.6	51.4	1.30
60.1	10.21	49.3	50.7	1.26
60.0	15.02	51.0	49.0	1.39
60.1	19.95	51.2	48.8	1.43

along with some data reported and measured previously [31] and data from Clark [1]. The data for all studies agree to within 0.2 mol% H_2O in the high-pressure liquid phase.

As was shown in Figure 2b, there is a lack of data for H_2S water content at reservoir pressures and the liquid H_2S data are principally those of Gillespie and Wilson [12]. Considering both these points, ASRL has modified its isolated floating piston vessels to achieve working pressures up to 100 MPa. The aim is to provide measurements for pure H_2S water contents at T = 50, 75 and 100°C for p < 100 MPa. In addition, a third cell has been constructed from titanium. This vessel may be used to measure the water content above brine for the same conditions. This is the current state of ASRL's high-pressure acid gas water content measurement capabilities and endeavors.

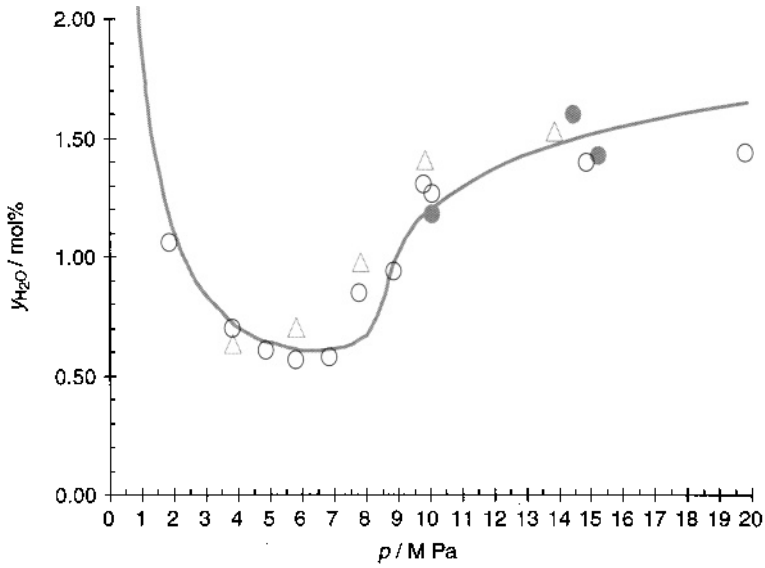

Figure 9. The Water Content of a 50:50 H_2S/CO_2 Mixture at $T = 60°C$.
•, early measurements by ASRL (2007); °, recent measurements by ASRL using the current isolated floating piston and microsampling apparatus (2009); △, M. A. Clark; [1] —, AQUAlibrium [8].

References

1. M. A. Clark, *Experimentally Obtained Saturated Water Content, Phase Behavior and Density of Acid Gas Mixtures*, MSc Thesis, University of Calgary (1999).
2. I. A. Alami, W. D. Monnery and W. Y. Svrcek, *Oil & Gas Journal* **103**(26), 48–54, (2005).
3. J. J. Carroll *J. Canadian Petroleum Technology* **41** (2002).
4. S. G. Jones, D. R. Rosa and J. E. Johnson *Oil & Gas Journal* **102**, 45–51, March 8 (2004).
5. J. J. Carroll, 81st GPA Convention, Dallas, TX, March 11–13 (2002).
6. J. R. Maddocks, M. Conacher and L. Dixon, SOGAT Proceedings, 235–253, May (2007).
7. VMGSim 2.8.0, Virtual Materials Inc., Calgary, AB.
8. AQUAlibrium 3.0, FlowPhase Inc., Calgary, AB.
9. A. Chapoy, A. H. Mohammadi, A. Chareton, B. Tohidi and D. Richon, *Ind. Eng. Chem. Res.* **43**, 1794–1802 (2004).
10. A. Chapoy, A. H. Mohammadi, B. Tohidi, A. Valtz and D. Richon, *Ind. Eng. Chem. Res.* **44**, 7567–7574 (2005).
11. R. Wiebe and V. L. Gaddy, *J. Am. Chem. Soc.* **63**, 475–477 (1941).
12. P. C. Gillespie and G. M. Wilson, *GPA Research Report RR-48*, Tulsa, OK (1982).
13. C. R. Coan and A. D. King Jr., *J. Am. Chem. Soc.* **93**, 1857–1862 (1971).

14. M. B. King, A. Mubarak, J. D. Kim and T. R. Bott, *J. Supercritical Fluids* **5**, 296–302 (1992).
15. A. Zawisza and B. Malesińska, *J. Chem. Eng. Data* **26**, 388–391 (1981).
16. R. D'Souza, J. R. Patrick and A. S. Teja, *Can. J. Chem. Eng.* **66**, 319–323 (1988).
17. A. Valtz, A. Chapoy, C. Coquelet, P. Paricaud and D. Richon, *Fluid Phase Equilibria* **226**, 333–344 (2004).
18. J. A. Briones, J. C. Mullins, M. C. Thies and B.-U. Kim, *Fluid Phase Equilibria* **36**, 235–246 (1987).
19. T. Nakayama, H. Sagara, K. Arai and S. Saito, *Fluid Phase Equilibria* **38**, 109–127 (1987).
20. R. Dohrn, A. P. Bünz, F. Devlieghere and D. Thelen, *Fluid Phase Equilibria* **83**, 149–158 (1993).
21. A. Bamberger, G. Sieder and G. Maurer, *J. Supercritical Fluids* **17**, 97–110 (2000).
22. J. J. Carroll and A. E. Mather, *Can. J. Chem. Eng.* **67**, 468–470 (1989).
23. F. T. Selleck, L. T. Carmichael and B. H. Sage, *Ind. Eng. Chem.* **44**, 2219–2226 (1952) [note that raw experimental data was plotted, not smoothed data].
24. S. S.-S. Huang, A.-D. Leu, H.-J. Ng and D. R. Robinson, *Fluid Phase Equilibria* **19**, 21–32 (1985).
25. R. Span and W. Wagner, *J. Phys. Chem. Ref. Data* **25**, 1509–1596 (1996).
26. I. P. Sidorov, Y. S. Kazarnovskii and A. M. Goldman, *Tr. GIAP* **1**, 48–67 (1952).
27. G. Müller, E. Bender andG. Maurer, *Ber Bunsen-Ges. Phys. Chem.* **92**, 148–160 (1988).
28. E. W. Lemmon and R. Span, *J. Chem. Eng. Data* **51**, 785–850 (2006).
29. R. H. Wright and O. Maass, *Can. J. Research.* **6**, 94–101 (1932).
30. J. I. Lee and A. E. Mather, *Ber Bunsen-Ges. Phys. Chem.* **81**, 1021–1023 (1977).
31. P. M. Davis, R. A. Marriott, E. Fitzpatrick, C. S. C. Lau and P. D. Clark, ASRL Chalk Talk, June 19th (2007) [tables included in proceedings].
32. E. Fitzpatrick, F. Bernard, R. A. Marriott and P. M. Davis, ASRL Chalk Talk, January 24th (2008).
33. U. K. Deiters and G. M. Schneider, *Fluid Phase Equilibria* **29**, 145–160 (1986).